FACTA UNIVERSITATIS (NIŠ)
Series: Electronics and Energetics vol. 14, No. 1 April 2001, 119-132

MODELING OF THE SAMPLING PROCESS FOR ALIASING SIGNAL EVALUATION IN A CCD CAMERA

Dragica Arandelović and Mile Petrović

Abstract: The paper deals with pre and post filtering with sampling processes discussion and modeling to determine the aliasing in a second generation CCD camera. A general explanation is followed by the practical examples. A new measure for aliasing contribution to signal is also derived, and signal to aliasing noise ratio is determined.

Key words: CCD sensor, optical sapling, point spread function, aliasing, aperture ratio.

1. Introduction

Generation of digital video signal in a modern TV camera requires A/D conversion of light excitation, which is always analog. CCD sensor is three-dimensional sampler of input optical signal. If sampling frequency is not chosen according to the Nyquist theorem, overlapping of upper bands with base band signal is the consequence. Therefore the useful signal will be mixed with false one that is not present in the original image. Implementation of optical lowpass filter in front of the CCD sensor significantly reduces aliasing but does not eliminate it.

The paper deals with sampling processes discussion and aliasing problem solution and determination. Prefiltering process for aliasing suppression and postfiltering process for signal reconstruction are discussed too.

Using the model aliasing signal evaluation and measurement can be done.

Manuscript received January 14, 2001.

D. Arandelović is with RTS Television Belgrade and Faculty of Drama Arts, Belgrade, Yugoslavia.

Dr. M. Petrović is with Faculty of Electrical Engineering, University of Priština, Yugoslavia (e-mail: milep@memodata.net).

2. CCD Sensor Sampling Processes

Although CCD sensor is the first step of the light signal digitalization, its output can not be inputted to the digital coder directly. Direct digitalization of CCD output is not possible because of: aliasing, noise and wide dynamic range which is still a problem even for the latest quantizers which are 12 bits.

Therefore, before digitalization, CCD output signal has to be processed in an analog block. For all new cameras it is usually said "full digital" but the word "full" relates to full digital processing excluding digital signal generation. As the digital processing block has to be preceded by A/D converter, another sampling process is implemented. Its sampling frequency is determined by previous block characteristics e.g. CCD sensor sampling structure.

CCD sensor used in a modern TV camera is a block with two main functions:

- three-dimensional sampling of optical input signal
- optoelectrical conversion CCD sampling process is divided in two steps:

(a) Optical sampling lattice - exact sampling

(b) electrical sampling lattice - square topped sampling for signal reconstruction and postfiltering

The sampling processes are based on aperture windows which are aligned with some pixel pitch (Fig. 1). Pixel dimensions ($\Delta x \times \Delta y$) and the pixel pitch values ($p_x \times p_y$) are determined by CCD sensor dimensions ($X \times Y$) and the total pixel number ($N_x \times N_y$).

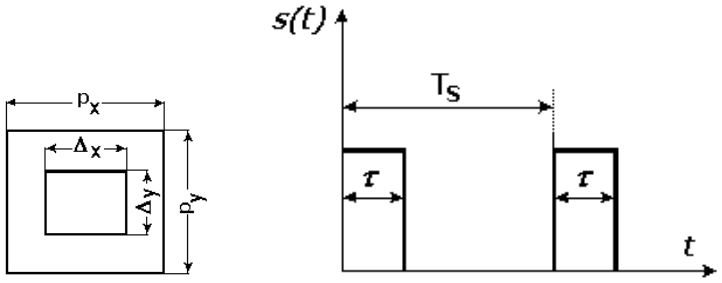

Fig. 1. (a) CCD sensor picture element - pixel.
(b) Picture element in time domain.

2.2 Optical sampling lattice - exact scanning

In the process of exact scanning, by definition, the modulated pulses follow the sampling function during the scanning interval.

Supposing pixel width, Δx, and sampling interval, p_x, frequency spectrum of the sampled signal is expressed by

$$F_{sop}(j\omega) = \theta_{sop} \sum_{n=-\infty}^{n=\infty} \frac{\sin(n\pi\theta_{sop})}{n\pi\theta_{sop}} \{F[j(\omega - n\omega_{sop}]\}, \tag{1}$$

where $\theta_{sop} = \Delta x/p_x$ is the optical sampling aperture ratio.

The effect of exact (optical) sampling is equivalent to multiplying the output spectrum $F[j(\omega - n\omega_{sop})]$ by a constant scale factor $\theta_{sop}\sin(n\pi\theta_{sop})/(n\pi\theta_{sop})$.

As an example we consider a cosine wave signal of period $2\pi/\kappa$:

$$f(x) = 1 + m\cos\kappa x, \tag{2}$$

with a frequency spectrum consisting of two spectral lines at $\omega \pm \kappa$ and an impulse function at the origin

$$F(j\omega) = 2\pi\delta(\omega) + m\pi\delta(\omega - \kappa) + m\pi\delta(\omega + \kappa). \tag{3}$$

So the frequency spectrum of the sampled signal is:

$$\begin{aligned} F_{sop}(j\omega) =& \theta_{sop} \sum_{n=-\infty}^{n=\infty} \frac{\sin(n\pi\theta_{sop})}{n\pi\theta_{sop}} \{2\pi\delta(\omega - n\omega_{sop}) \\ &+ m\pi[\delta(\omega - \kappa - n\omega_{sop}) + m\pi[\delta(\omega - \kappa - n\omega_{sop})]\} \end{aligned} \tag{4}$$

or

$$F_{sop}(j\omega) = S(j\omega) + m\theta_{sop}\pi \sum_{n=-\infty}^{n=\infty} \frac{\sin(n\pi\theta_{sop})}{n\pi\theta_{sop}} \delta[\omega - (n\omega_{sop} \pm \kappa)], \tag{5}$$

where $S(j\omega)$ represents spectrum of the scanning pulses and the remaining terms represent the sidebands about the harmonics of the scanning frequency.

Second example is test chart that is used for TV resolution measurement. It is made of black and white stripes of different width i.e. different

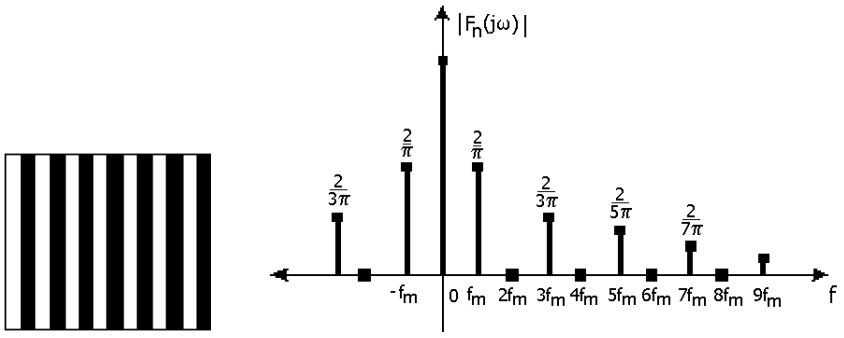

Fig. 2. (a) Test chart for TV resolution measurement. (b) Frequency spectrum for test chart..

frequencies (Fig. 2). One black and one white stripe represent one line pair and, by convention, 80 line pairs per picture width (lp/ppw) correspond to frequency of 1 MHz.

Suppose that in front of the camera is the chart consisting of black and white stripes of frequency f_m. As the input excitation is equivalent to rectangular pulse of duration τ_m, and period $T_m = 1/f_m$, it can be expressed by

$$f(t) = \frac{\tau_m}{T_m}\Big[1 + 2\sum_{k=1}^{\infty} \frac{\sin\dfrac{k\omega_m\tau_m}{2}}{\dfrac{k\omega_m\tau_m}{2}} \cos(k\omega_m t)\Big], \tag{6}$$

where T_m is period and $\omega_m = 2\pi f_m = 2\pi/T_m$ is the fundamental angle frequency of the signal.

The frequency spectrum of the input signal displayed on Fig. 2(b), can be expressed by the following equation

$$F(j\omega) = \pi\Big\{\delta(\omega) + \sum_{k=1}^{\infty} \frac{\sin\dfrac{k\pi}{2}}{\dfrac{k\pi}{2}} [\delta(\omega - k\omega_m) + \delta(\omega + k\omega_m)]\Big\}. \tag{7}$$

It follows that frequency spectrum of the sampled signal is:

$$F_{sop}(j\omega) = \pi\theta_{sop} \sum_{n=-\infty}^{\infty} \frac{\sin(n\pi\theta_{sop})}{n\pi\theta_{sop}} \Big\{ \delta(\omega - n\omega_{sop}) + \sum_{k=1}^{\infty} \frac{\sin\frac{k\pi}{2}}{\frac{k\pi}{2}} [\delta(\omega - k\omega_m - n\omega_{sop}) + \delta(\omega + k\omega_m - n\omega_{sop})] \Big\}. \tag{8}$$

The frequency spectrum of input excitation is almost infinite, so overlapping of sidebands is unavoidable and aliasing is evident. Implementation of optical low pass filter in front of the CCD sensor significantly reduces aliasing but does not eliminate it. Supposing that cutoff frequency of the low pass filter is f_g, aliasing causes the k-th input signal component in n-th sideband given by the following expressions

$$\begin{aligned} nf_s - kf_m &\leq f_g, \\ k &\geq \frac{nf_s - f_g}{f_m}, \end{aligned} \tag{9}$$

where f_m is the input signal base frequency, f_s is sampling frequency, f_g is low pass filter cutoff frequency.

2.3 Electrical sampling lattice - square topped scanning

In the process of electrical sampling for signal reconstruction, the sampled signal pulses do not follow the sampled time function $f(t)$ during the scanning interval. The value of $f(t)$ which corresponds to the center, or any other fixed reference position of the pulse, is effective in the sampling process.

The sampled signal is expressed by

$$f_s(t) = \sum_{n=-\infty}^{n=\infty} f(nT)s(t - nT), \tag{10}$$

where

$$s(t) = \begin{cases} 1, & -\frac{\tau_{sel}}{2} < t < \frac{\tau_{sel}}{2} \\ 0, & \text{elsewere.} \end{cases} \tag{11}$$

The resulting frequency spectrum of sampled signal is

$$F_{sel}(j\omega) = \frac{\tau_{sel}}{T_{sel}} \frac{\sin\frac{\omega\tau_{se}}{2}}{\frac{\omega\tau_{sel}}{2}} \sum_{n=-\infty}^{\infty} F[j(\omega - n\omega_{sel}] \tag{12}$$

As we can see, the amplitude of the resulting frequency spectrum is not constant in the signal band. So, we conclude that electrical sampling introduces frequency dependent distortion.

We can compare Eq. (12) with the spectrum of the exact sampling signal. The spectrum of optically sampled signal consists of sidebands obtained by frequency translation of original signal. Translation is done for all multiple of sampling frequency. For electrical sampling there are such translations, but the MTF of each sideband located at 0, ω_{sel}, $2\omega_{sel}$, $3\omega_{sel}$ is modified by factor $\sin(\omega\tau_{sel}/2)/\omega\tau_{sel}/2$.

that is dependent on frequency, what was not the case for optical sampling. Low pass filter performs signal reconstruction, but the obtained signal will be distorted. The use of an equalizer after the low pass filter can reduce the distortion.

2.4 Practical realization

Practical realization of optical sampling is represented by integration process (Fig. 3). For the case of cosine input excitation sampled signal is

$$\begin{aligned} f_l(lp_{xop}) =& \frac{1}{\Delta x_{op}} \int_{lp_{xop}-\frac{\Delta x_{op}}{2}}^{lp_{xop}+\frac{\Delta x_{op}}{2}} [1+\cos(\kappa x)]dx \\ =& 1 + \frac{\sin\frac{\kappa\Delta x_{op}}{2}}{\frac{\kappa\Delta x_{op}}{2}} \cos(\kappa l p_{xop}), \end{aligned} \tag{13}$$

where Δx_{op} is optical aperture size, p_{xop} is optical pixel pitch and l is an integer number, $-N \leq l \leq N$.

In the process of electrical sampling in sample and hold block for signal reconstruction, pulse widening is done. So pixel size becomes equal to pixel pitch ($p_{xel} = p_{xop}$).

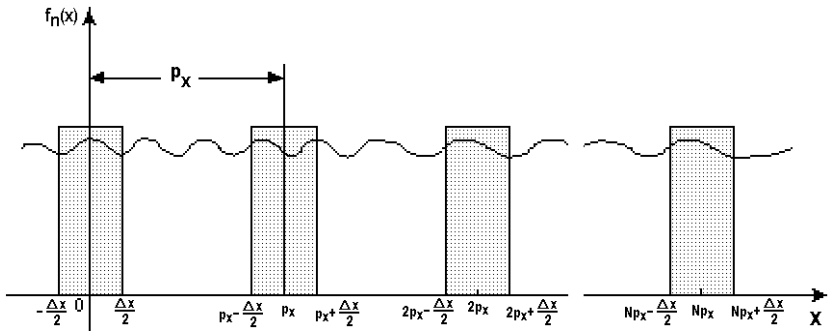

Fig. 3. Integration process.

In the reconstruction process signal component $f_l(lp_{xop})$ is multiplied by sample and hold pulse $s(x)$, and summing process is done. So reconstructed signal is

$$f(x) = \sum_{l=-N}^{N} \left[1 + \frac{\sin\frac{\kappa\Delta x_{op}}{2}}{\frac{\kappa\Delta x_{op}}{2}} \cos(\kappa l p_{xop})\right] s(x - lp_{xel}), \tag{14}$$

where $2N + 1$ is the total pixel number.

Spectral distribution of reconstructed signal is obtained by Furrier transformation

$$\begin{aligned} F(\omega_x) &= \int_{-\infty}^{\infty} f(x) e^{-j\omega_x x} dx \\ &= \sum_{l=-N}^{N} \left[1 + \frac{\sin\frac{\kappa\Delta x_{op}}{2}}{\frac{\kappa\Delta x_{op}}{2}} \cos(\kappa l p_{xop})\right] \int_{-\infty}^{\infty} s(x - lp_{xel}) e^{-j\omega_x x} dx. \end{aligned} \tag{15}$$

As

$$\int_{-\infty}^{\infty} s(x - lp_{xel}) e^{-j\omega_x x} dx = p_{xel} \frac{\sin\frac{\omega_x p_{xel}}{2}}{\frac{\omega_x p_{xel}}{2}} e^{-jlp_{xel}\omega_x} \tag{16}$$

and geometric series sum is

$$\sum_{l=-N}^{N} e^{-jlp_x\omega_x} = (2N+1)\frac{\sin\dfrac{(2N+1)\omega_x p_x}{2}}{\dfrac{(2N+1)\omega_x p_x}{2}}\left[\frac{\sin\dfrac{\omega_x p_x}{2}}{\dfrac{\omega_x p_x}{2}}\right]^{-1}, \qquad (17)$$

then in the reconstruction process pulse widening is done, and p_{xop} is equal to p_{xel} so the frequency spectrum of the reconstructed signal is

$$\begin{aligned} F(\omega_x) = p_x \frac{\sin\dfrac{\omega_x p_x}{2}}{\dfrac{\omega_x p_x}{2}}\Bigg\{ & \sum_{l=-N}^{N} e^{-jlp_x\omega_x} \\ & + \frac{\sin\dfrac{\kappa\Delta x}{2}}{\dfrac{\kappa\Delta x}{2}}\left[\sum_{l=-N}^{N} e^{-jlp_x(\omega_x-\kappa)} + \sum_{l=-N}^{N} e^{-jlp_x(\omega_x+\kappa)}\right]\Bigg\} \end{aligned} \qquad (18)$$

And finaly

$$\begin{aligned} F(\omega_x) = & p_x \frac{\sin\dfrac{\omega_x p_x}{2}}{\dfrac{\omega_x p_x}{2}}\Bigg\{(2N+1)\frac{\sin\dfrac{(2N+1)\omega_x p_x}{2}}{\dfrac{(2N+1)\omega_x p_x}{2}}\left[\frac{\sin\dfrac{\omega_x p_x}{2}}{\dfrac{\omega_x p_x}{2}}\right]^{-1} \\ & + \frac{\sin\dfrac{\kappa\Delta x}{2}}{\dfrac{\kappa\Delta x}{2}}\Bigg[(2N+1)\frac{\sin\dfrac{(2N+1)(\omega_x-\kappa)p_x}{2}}{\dfrac{(2N+1)(\omega_x-\kappa)p_x}{2}}\left[\frac{\sin\dfrac{(\omega_x-\kappa)p_x}{2}}{\dfrac{(\omega_x-\kappa)p_x}{2}}\right]^{-1} \\ & + (2N+1)\frac{\sin\dfrac{(2N+1)(\omega_x+\kappa)p_x}{2}}{\dfrac{(2N+1)(\omega_x+\kappa)p_x}{2}}\left[\frac{\sin\dfrac{(\omega_x+\kappa)p_x}{2}}{\dfrac{(\omega_x+\kappa)p_x}{2}}\right]^{-1}\Bigg]\Bigg\} \end{aligned} \qquad (19)$$

Graph of the obtained result for $p_x = 72$ ns, $\Delta x = 24$ ns, $N = 360$ and $\kappa = 2\pi 250$ rad/s, is shown in Fig. 4.

3. Low Pass Filter

It has been already noted that optical low pass filter, implemented in front of the CCD sensor, reduces side bands overlapping.

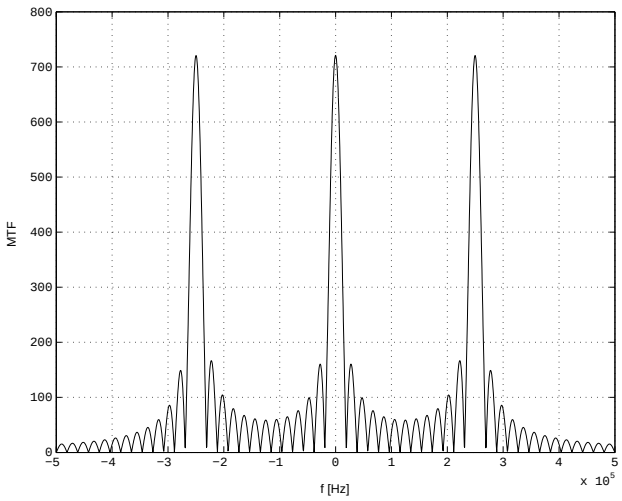

Fig. 4. Graph of the function obtained by Equation (19).

The optical prefilter consisting of one or more quartz crystal plates (Savart's plate), utilizes double refraction characteristic of Savart's plate (Fig. 5(a)). Incident beam is separated at two or more points with the same luminous intensity. Point spread function and modulation transfer function) of the filter are determined by crystal plates number (n), plate thickness (t_h) and angle between crystal axes (α).

The choice of filter structure depends on CCD sensor type and camera quality. Very high studio quality cameras have complex filters with good characteristics in horizontal, vertical and diagonal direction. Fig. 5(b) show some special filter structure used in higher quality cameras.

Impulse response of filter that is shown in Fig. 5(b) can be expressed by the following equation

$$\begin{aligned} h(x,y) =& \frac{1}{2}\delta(x-\frac{d_x}{2}, y-\frac{d_y}{2}) + \frac{1}{2}\delta(x+\frac{d_x}{2}, y-\frac{d_y}{2}) + \frac{1}{2}\delta(x-d_x, y-\frac{d_y}{2}) \\ &+\delta(x, y-\frac{d_y}{2}) + \frac{1}{2}\delta(x+d_x, y-\frac{d_y}{2}) + \frac{1}{2}\delta(x-\frac{d_x}{2}, y) + \delta(x+\frac{d_x}{2}, y) \\ &+\frac{1}{2}\delta(x-d_x, y-\frac{d_y}{2}) + \delta(x, y+\frac{d_y}{2}) + \frac{1}{2}\delta(x+d_x, y+\frac{d_y}{2}) \\ &+\frac{1}{2}\delta(x-\frac{d_x}{2}, y+\frac{d_y}{2}) + \frac{1}{2}\delta(x+\frac{d_x}{2}, y+\frac{d_y}{2}) \end{aligned} \tag{20}$$

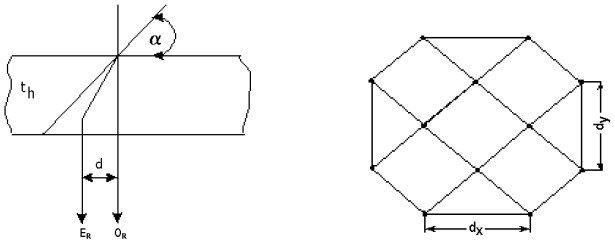

(a) (b)

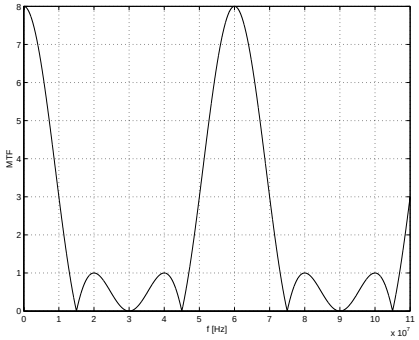

(c)

Fig.5. (a) Crystal plate (simple filter).
(b) Orthogonal filter structure.
(c) Modulation transfer function in horizontal direction.

Frequency response of the filter is

$$H(\omega_x, \omega_y) = 8 \cos \frac{\omega_x d_x}{2} \cos \frac{\omega_y d_y}{2} \cos \frac{\omega_x d_x + \omega_y d_y}{4} \cos \frac{\omega_x d_x - \omega_y d_y}{4} \quad (21)$$

Modulation transfer function in horizontal direction is

$$MTF_h = |H(\omega_x, 0)| = 8 \left| \cos \frac{\omega_x d_x}{2} \cos^2 \frac{\omega_x d_x}{4} \right| \quad (22)$$

Plot of modulation transfer function is shown in Fig. 5(c).

3.2 Aliasing

Using the previous discussion and the proposed models, aliasing noise can be determined. The analysis is done using the Fig. 6.

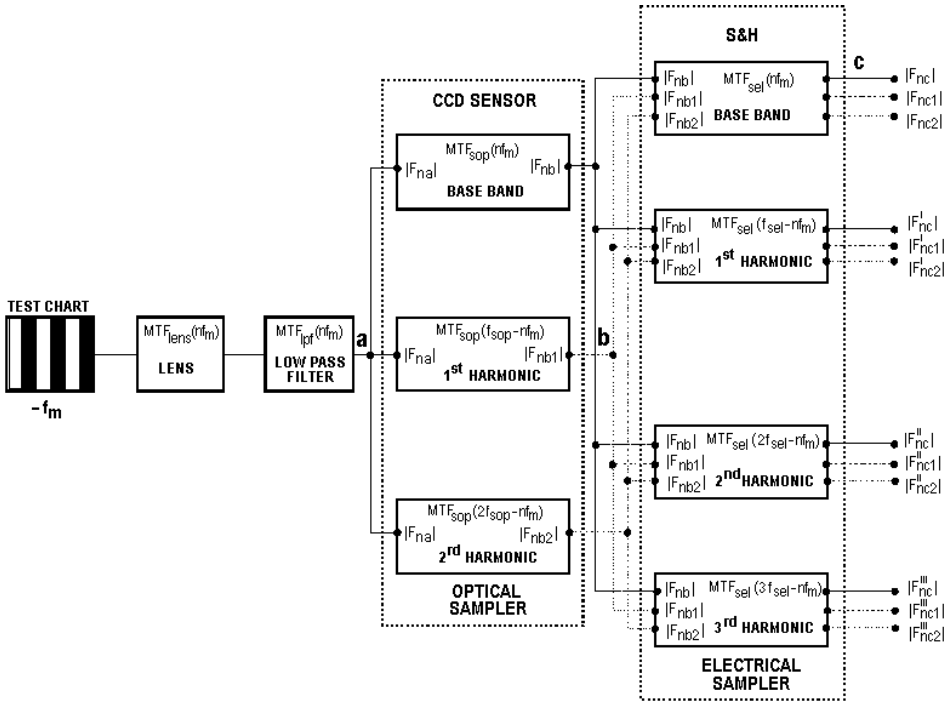

Fig. 6. Aliasing noise model.

Input signal is the test chart shown in Fig. 5 with the frequency spectrum determined by the base frequency f_m and amplitude response $|F_n|$. The signal is passed through low pass filter with modulation transfer function MTF_{LPF} so the signal in point **a** is $|F_{na}| = |MTF_{LPF}(nf_m)$. For the case of the chart the value of F_n is given by Eq. (7).

Then signal passes optical sampling block in CCD sensor with the response determined by aperture ratio θ_{sop}. Signal at point B is optically sampled signal so it consists of useful signal (base band) and undesirable components caused by mirroring of higher order harmonics into base band (aliasing).

Signal at point **b** is:

- Base band signal $|F_{nb}| = |F_{nb}(nf_m)| = |F_{na}|MTF^0_{sop}$
- 1-st harmonic of CCD out signal (aliasing source) $|F_{nb_1}| = |F_{na}(f_{sop} - nf_m)|MTF^1_{sop}$.

- 2-nd harmonic of CCD out signal (aliasing source) $|F_{nb_2}| = |F_{nb}(2f_{sop} - nf_m)|MTF^2_{sop}$.

Then signal passes to electrical sampling block represented by sample and hold circuit that resamples signal. It samples base band signal $|F_{nb}|$, but it also samples the higher order harmonics what gives new aliasing components which are not present at Optical sampler out.

The sample and hold block out signal at point **c** is base band signal $|F_{nc}| = F_{nc}(nf_m)| = |F_{nb}| = |F_{nb}(nf_m)|MTF_{sel}(nf_m)$.

Electrical sampling of higher order harmonics at optical block output, influences new aliasing components:

- Resampling of optical sampler out 1-st harmonic $|F_{nc_1}| = |F_{nb_1}| \times MTF_{sel}(f_{sop} - nf_m)$
- Resampling of optical sampler out 2-nd harmonic $|F_{nc_2}| = |F_{nb_2}| \times MTF_{sel}(2f_{sop} - nf_m)$
- Resampling of optical sampler out 3-rd harmonic $|F_{nc_3}| = |F_{nb_3}| \times MTF_{sel}(3f_{sop} - nf_m)$, where $|F_{nc_i}|$, $i = 1, 2, 3$, means i-th harmonic of optical sampler out is electrically sampled and gives components in base band signal.

Higher order harmonics of electrical sampler out signal cause new aliasing components:

$$\begin{aligned}
|F^I_{nc}| &= |F_{nb}|MTF_{el}(f_{sel} - nf_m) \\
|F^I_{nc_1}| &= |F_{nb_1}|MTF_{el}(f_{sel} - nf_m) \\
|F^I_{nc_2}| &= |F_{nb_2}|MTF_{el}(f_{sel} - nf_m) \\
&\vdots \\
|F^I_{nc_N}| &= |F_{nb_N}|MTF_{el}(f_{sel} - nf_m),
\end{aligned}$$

where $|F_{nbi}|$ is i-th harmonic of CCD out signal and $|F^k_{nc1}|$ is k-th harmonic of sample and hold block out obtained by sampling of 1-st harmonic of CCD out.

Similarly, 2-nd harmonic of sample and hold circuit out contains the following aliasing components:

$$\begin{aligned}
|F^{II}_{nc}| &= |F_{nb}|MTF_{el}(2f_{sel} - nf_m) \\
|F^{II}_{nc_1}| &= |F_{nb_1}|MTF_{el}(2f_{sel} - nf_m) \\
|F^{II}_{nc_2}| &= |F_{nb_2}|MTF_{el}(2f_{sel} - nf_m)
\end{aligned}$$

Base band signal and higher order harmonics at the sample and hold circuit output are shown in Fig. 6. From sample and hold block signal passes to Amplifier and CDS block. Magnitude transfer function of CDS (Correlated Double Sampling) and amplifier is

$$MTF_{CDS}MTF_{AMP} = \left(1 - \cos\frac{\pi f}{f_{se}}\right)\left(1 + \frac{f}{f_{AMP}}\right) \tag{23}$$

where f_{AMP} is 3dB cutoff frequency of amplifier.

If point **d** is output at CDS (Correlated Double Sampling) and PA (Preampifier) blok then signal at point **d** is

$$|F_{nd}| = |F_{nc}|MTF_{CDS}MTF_{AMP}.$$

By the Parselval's theorem power spectrum of the useful output signal is

$$S_{11}(n\omega_0) = \sum |F_{nd}|^2$$

Power spectrum of aliasing components is

$$S_{al}(n\omega_0) = \sum |F_{ndi}|^2 + \sum |F^I_{ndi}|^2 + \sum |F^{II}_{ndi}|^2$$

We define Signal to Aliasing Ratio (SAR), as a measure for aliasing contribution to signal

$$SAR = 10\log\frac{S_{11}(n\omega_0)}{S_{al}(n\omega_0)}.$$

4. Conclusion

In the study the analysis of CCD camera optical block and sampling process modeling has been presented. Sampling process introduces aliasing that causes serious problems in a modern digital cameras. It is visible in the picture as a moiré and as bit patterning on high frequencies. It is also an important noise source that influences problems in the following digitalization circuit.

Optical low pass filters are discussed and some filter characteristics are given. Their influence on camera quality is shown.

The model and the proposed sampling process analysis can be developed for new camera measurement and camera aliasing evaluation.

REFERENCES

1. V. Krasnjuk, D. Arandjelovic, M. Petrovic, and M.Hribsek: *A CCD model applied to colour camera characteristics measurement.* In: Proc. IEE Conference Publication No. 397, Amsterdam IBC 1994, pp. 411 - 415.
2. V. Krasnjuk, M. Petrovic, and D. Arandjelovic: *Dynamic range of CCD camera.* In: Proc. 6th Int. Conference on Television Techniques 1994, Budapest, Hungary.
3. P. Centeen: *Dynamic pixel management for second generation aspect ratio switching.* In: Proc. 19th Int. Television Symposium, Montreux 1995.
4. I. Roou, R. Voet, B. Botte, J.P. Lacoste, and K. Behinda: *Requirements for digital signal processing in broadcast cameras.* In: Proc. 19th Int. Television Symposium, Montreux 1995.
5. Sony Broadcast International: *A second generation HDTV camera using a two million pixel CCD.* In: Proc. 18th Int. Television Symposium, Montreux 1995.
6. V. Krasnjuk, D. Arandjelovic, M. Petrovic, and M. Hribsek: *Mathematical modeling of prefiltering and postfiltering process in a CCD camera.* In: Proc. Int. Workshop on HDTV, Los Angeles 1996.